Acta Materialia 216 (2021) 117150

Contents lists available at ScienceDirect

Acta Materialia

journal homepage: www.elsevier.com/locate/actamat

Full length article

A half-shear-half-shuffle mechanism and the single-layer twinning dislocation for $\{11\bar{2}2\}\langle 11\bar{2}\bar{3}\rangle$ mode in hexagonal close-packed titanium

Jingwei Li[a], Manling Sui[a,*], Bin Li[b,*]

[a] Beijing Key Laboratory of Microstructure and Properties of Solids, Faculty of Materials and Manufacturing, Beijing University of Technology, Beijing 100124, China

[b] Department of Chemical and Materials Engineering, University of Nevada, Reno, NV 89557, USA

ARTICLE INFO

Article history:
Received 11 May 2021
Revised 29 June 2021
Accepted 30 June 2021
Available online 6 July 2021

Keywords:
Lattice correspondence
Twin boundary
Twinning dislocation

ABSTRACT

Among the twinning modes in hexagonal close-packed (HCP) metals, the mechanism for $\{11\bar{2}2\}\langle 11\bar{2}\bar{3}\rangle$ mode is particularly confusing and controversial. In the literature reports, there are three possible second invariant planes, i.e. the K_2 planes for $\{11\bar{2}2\}\langle 11\bar{2}\bar{3}\rangle$ twinning mode: $\{11\bar{2}\bar{4}\}$ which has been widely accepted and corresponds to a three-layer zonal twinning dislocation; $\{11\bar{2}\bar{2}\}$ that is deemed unfavorable; and (0002) which has only been observed in atomistic simulations and corresponds to a single-layer twinning dislocation. $\{11\bar{2}\bar{4}\}$ was predicted by classical twinning theory and the experimentally measured magnitude of twinning shear s in titanium and zirconium seemed to agree well with the prediction. However, $\{11\bar{2}\bar{4}\}$ has never been verified in simulations which show that (0002) should be the K_2 plane. This conflict has not been resolved due to the lack of experimental observation of the structure of twinning dislocations. In this work, scanning transmission electron microscopy (STEM) observations are conducted to resolve the twin boundary structure in deformed pure titanium on the atomic scale, combined with atomistic simulations. Atomic resolution STEM unambiguously shows that the twinning dislocation only involves a single twinning plane and the K_2 plane is (0002), which is consistent with the atomistic simulations. The STEM results also reveal a half-shear-half-shuffle process which is manifested by a unique twin boundary structure generated by the glide of single-layer twinning dislocations. To explain these results, the lattice correspondences of all three K_2 planes are examined in great detail. In particular, shear and shuffle required in the lattice transformations are analyzed inside the framework of classical theory. These analyses explain well why (0002) is the more favorable K_2 plane than $\{11\bar{2}\bar{4}\}$ and $\{11\bar{2}\bar{2}\}$, and properly resolve the conflict between the prediction of the classical twinning theory and the simulation results.

1. Introduction

$\{11\bar{2}2\}\langle 11\bar{2}\bar{3}\rangle$ twinning mode has been observed in hexagonal close-packed (HCP) titanium (Ti) and zirconium (Zr). It is an important deformation mode when crystals are compressed along the *c*-axis [1–13], but the mechanism for this twinning mode has not been fully understood. Confusing even contradicting reports can be found in the literature. As shown in Fig. 1, there are three possible K_2 planes in the literature reports: (i) $\{11\bar{2}\bar{4}\}$. This K_2 plane was predicted in the classical twinning theory [14,15]. Its corresponding magnitude of twinning shear s equals ~0.22 for Ti. (ii) $\{11\bar{2}\bar{2}\}$, which was proposed by Hall [16]. (iii) (0002), i.e. the basal plane [17,18]. This K_2 plane was not predicted to be possible in the classical twinning theory because the value of s of this K_2 plane would seemingly be 1.26 for Ti, which is larger than 1.0. According to Christian and Mahajan [15], the s of a twinning mode should be less than 1.0. From Fig. 1, s is associated with the acute angle θ between the K_2 and the K_2' by: $s = 2tan\frac{\theta}{2}$ [19]. Thus, it can be seen that K_2 = (0002) appears to have the largest value of s, and K_2= $\{11\bar{2}\bar{4}\}$ has the smallest among the three K_2 planes.

The predicted twinning elements can be verified by experimentally measuring the value of s. If the measured s is close to the predicted value, then the corresponding K_2 is correct. Traditionally, the value of s of a twinning mode was measured by using interferometry, for example, the measured value of s for $\{11\bar{2}2\}$ mode in Ti and Zr was close to 0.22 [1,2]. Naturally, this seems to confirm that the predicted K_2 plane by the classical theory, $\{11\bar{2}\bar{4}\}$, is correct, and the corresponding twinning dislocation should comprise three $\{11\bar{2}2\}$ twinning planes simultaneously, i.e. a three-layer zonal twinning dislocation [15]. Westlake [20] made a similar description

* Corresponding author.
E-mail addresses: mlsui@bjut.edu.cn (M. Sui), binl@unr.edu (B. Li).

https://doi.org/10.1016/j.actamat.2021.117150
1359-6454/

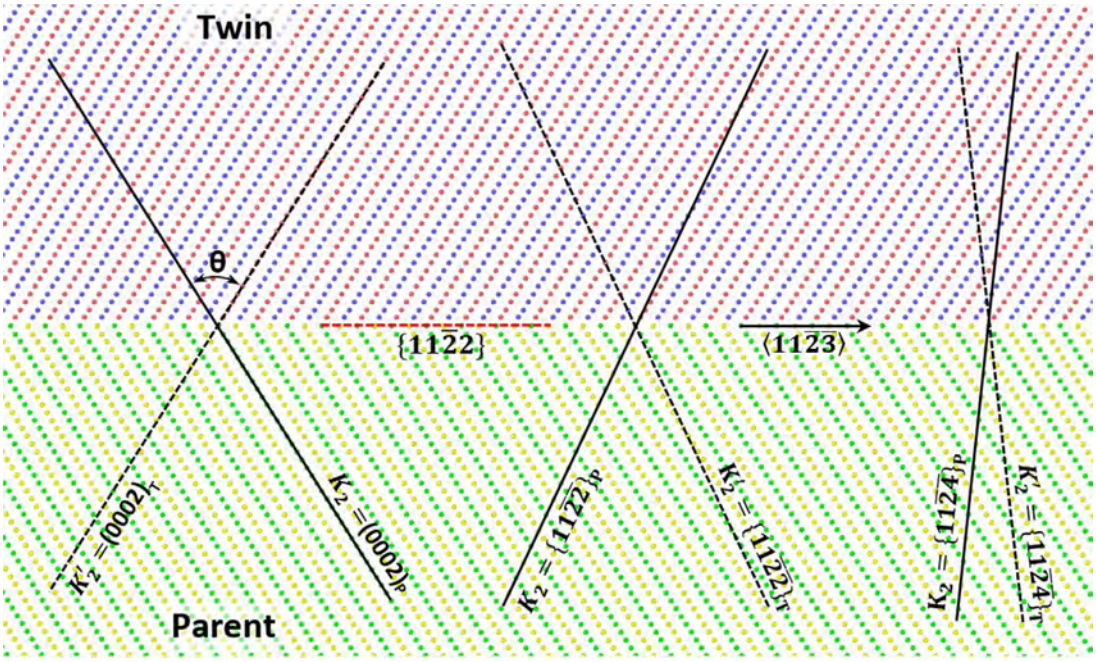

Fig. 1. Initial configuration of {11$\bar{2}$2}⟨11$\bar{2}$3⟩ twins. Zone axis ⟨1$\bar{1}$00⟩. The basal planes of the parent and the twin are colored differently to better show lattice transformation during twinning. Three K_2 planes reported in the literature, i.e. {0002} [17], {11$\bar{2}\bar{2}$} [16] and {11$\bar{2}\bar{4}$} [15] are indicated by the solid lines which extend from the parent into the twin, and the corresponding $K_2^{'}$ planes are indicated by the dashed lines which extend from the twin into the parent. The magnitude of twinning shear s, reflected by the acute angle θ between the K_2 and the $K_2^{'}$, decreases from left to right.

that "a homogeneous shear occurs on every third plane", but atoms in the two planes between composition planes had to move out of the plane of shear {1$\bar{1}$00}, i.e. the plane comprising the direction of twinning shear and the twinning plane normal. Christian and Mahajan [15] and Westlake [20] suggested that complicated shuffles should be involved. But so far, no complete analysis of shuffles has been provided if the K_2 plane is indeed {11$\bar{2}\bar{4}$}.

Although the experimental value of s (~0.22) seems to agree with the prediction of the classical theory, a conflict arises: in molecular dynamics (MD) simulations, the predicted K_2 has not been observed, but rather, the K_2 plane in the simulations is always (0002). For example, Serra et al. [17] simulated TB migration in α-Ti using a Finnis-Sinclair potential and found that the K_2 plane was (0002) and the TB migrated via glide of single-layer twinning dislocations. Serra and Bacon [18] investigated the twinning mechanism for {11$\bar{2}$2} mode in zirconium (Zr). They first constructed a three-layer disconnection at the twin boundary (TB) and then simulated how the TB migrated when a shear strain was applied parallel to the TB. Interestingly, the constructed three-layer disconnection was immobile. Instead, one-layer twinning dislocations were nucleated and glided on the TB. For the one-layer twinning dislocations, the corresponding K_2 plane was (0002), rather than {11$\bar{2}\bar{4}$}. The K_2 plane obtained from their MD simulations, (0002), appears to be the least possible because, from Fig. 1, this K_2 plane seemingly has the largest s = 1.26, which is larger than 1.0. But in the classical theory, the s of a twinning mode should be less than 1.0. Serra and Bacon [18] also reported that an artificially constructed three-layer dislocation $b_{\pm3}$ on the TB was immobile and its glide was "temperature dependent", whereas the single-layer dislocation $b_{\pm1}$ was mobile and temperature independent. The mobile $b_{\pm1}$ and the immobile $b_{\pm3}$ reacted to form a ⟨c + a⟩ dislocation. Single-layer twinning dislocations for {11$\bar{2}$2}⟨11$\bar{2}$3⟩ in Ti were also obtained by Li et al. [21] in their MD simulations. Again, the corresponding K_2 plane was (0002). Each twinning dislocation glided on a single twinning plane, rather than the predicted zonal dislocation spread on three consecutive twinning planes. Note that Ti and Zr have similar c/a ratios (1.588 for Ti and 1.593 for Zr), and similar twinning mechanism should be expected for the {11$\bar{2}$2} mode in these metals.

To reconcile the conflict between the predicted K_2= {11$\bar{2}\bar{4}$} and the K_2= (0002) obtained in their simulation, Serra et al. [18,22] claimed that {11$\bar{2}$2}⟨11$\bar{2}$3⟩ twinning mode had two different K_2 planes, depending on the direction of the resolved shear stress on the twin boundary; when the direction was reversed, the K_2 plane switched from (0002) to {11$\bar{2}\bar{4}$}, and the twinning dislocation switched from $b_{\pm1}$ to $b_{\pm3}$. However, this is not possible because any twinning mode can only have a unique K_2 plane and a unique lattice correspondence. Barrett and El Kadiri [23] also observed in their simulation that the twinning dislocation was not a three-layer zonal, instead, a single-layer dislocation. But they claimed that the single-layer twinning dislocations in their work and in the others were "artifacts" [24]. The fact that all the atomistic simulations ended up with the same single-layer twinning dislocation rather than the predicted three-layer zonal, and the same K_2 plane of (0002) strongly suggests that important factors were likely overlooked in previous works and more investigation is needed in order to fully resolve the twinning mechanism.

To summarize, there have been controversial reports on the mechanism of {11$\bar{2}$2}⟨11$\bar{2}$3⟩ twinning in the literature [18,21–24]. If the prediction of the classical theory is correct, then the twinning elements obtained from the MD simulations are false. But if the simulation results are correct, then these results suggest that the prediction of the classical theory is inaccurate, and the measured s is inaccurate as well and some sources of error in those experiments might have been neglected. But a lingering question will have to be addressed: how can it be possible that the seemingly implausible K_2 = (0002), which gives a value of s exceeding 1.0, defies the classical theory and is actually the K_2 plane?

In this work, atomic resolution scanning transmission electron microscopy (STEM) analysis of {11$\bar{2}$2} TB structure in pure Ti, and atomistic simulations of TB migration are conducted to resolve the {11$\bar{2}$2} twinning mechanism with clarity. Comprehensive lat-

tice correspondence analyses of all three reported K_2 planes are provided, in great detail, and these analyses are compared with experimental and simulation results. These results unambiguously verify that the K_2 plane is indeed (0002).

2. Experimental and simulation methods

The material used in the experiment was commercially pure Ti (99.99 at.%) with an average grain size of about 30 μm. The as-received material contains no deformation twins before deformation. A rectangular slab with dimensions of 50 mm × 20 mm × 8 mm was cut and annealed at 873 K for 4 h and then cooled in the furnace. After annealing, the slab was cold rolled multiple times at room temperature. For each pass the thickness reduction was ~ 200 μm and the total reduction rate was 30%. The rolled sample was sliced into thin sheets with a thickness about 500 μm, parallel to the plane that contains the rolling direction (RD) and the normal direction (ND). The thin sheets were mechanically ground to 60 μm and then punched into 3 mm discs. The discs were then further thinned by using a twin-jet electrochemical polisher with a solution of 14 vol.% sulphuric acid and 86 vol.% methanol. The polishing temperature was 243 K at an applied voltage of 25 V. Scanning transmission electron microscopy (STEM) characterization was performed by using a Cs-corrected FEI Titan G2 60–300 transmission electron microscope operated at 300 kV.

To better understand the twinning mechanism, MD simulations were also conducted in this work. Embedded Atom Method (EAM) potential for Ti and Al binary systems [25] was used for the simulations [26,27]. This potential was used in a number of previous simulations [21,24]. $\{11\bar{2}2\}\langle 11\bar{2}\bar{3}\rangle$ twins were first created by bonding together two single crystals which satisfied $\{11\bar{2}2\}$ twin relationship (Fig. 1). After the twins were created, the system was relaxed for 20 ps. The initial twins are shown in Fig. 1 with the viewing direction along $\langle 1\bar{1}00\rangle$. The system had dimensions of 40 nm × 40 nm × 40 nm, and the total number of particles was ~ 2.6 million. In previous simulations [21], the system thickness was about half of that in the present work, and the morphology of the twinning dislocations appeared to be pairs of arcs that were nucleated on the free surface. It was anticipated that if the system size was increased, the arcs would become dislocation loops [21].

No periodic boundary condition was applied in any dimension. The time step size was 4.0 *fs*. After relaxation, a shear strain was applied parallel to the twinning plane. To generate a constant strain rate, a constant displacement rate was assigned to the top surface of the system, which produced a strain rate about 2.1×10^8 s^{-1}. A constant temperature 10 K was maintained by applying the Nosé–Hoover [30,31] thermostat to the system during shear deformation. Atomistic simulation package XMD was used in this work.

The unrelaxed twin structure shown in Fig. 1 comprises a thin slice (0.6 nm) taken along the zone axis $[1\bar{1}00]$. In this edge-on view along the zone axis, a special coloring technique is used. The basal planes of the parent crystal are "dyed" in green and yellow alternately to represent the alternate basal stacking, whereas the basal planes of the twin crystal in red and blue. The initial TB is denoted by the dashed red line. During the simulation, the color of each atom remains unchanged. This special technique allows one to easily resolve lattice transformation during twinning, which is a crucial feature in deformation twinning [28]. As stated by Christian [29], during twinning, a crystallographic or atomic plane of the parent lattice must be transformed to a corresponding plane of the twin lattice. The color scheme greatly facilitates convenient identification of such transformations.

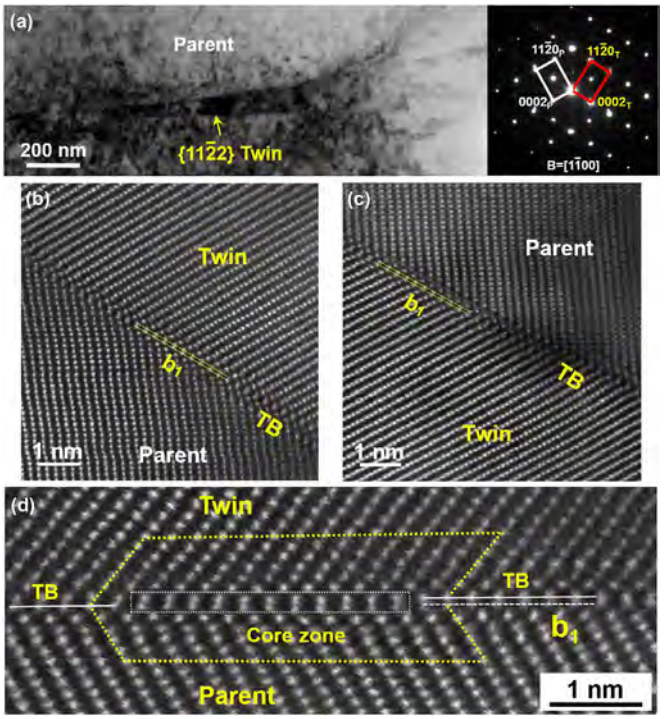

Fig. 2. (a) Low magnification TEM image of a $\{11\bar{2}2\}$ twin in deformed pure Ti. (b) and (c) Atomic resolution STEM images of $\{11\bar{2}2\}$ twin boundary structure. Only one twinning plane is involved in migration. (d) A magnified view of the twinning dislocation. A circuit of dotted yellow lines is drawn to show that the twinning dislocation only involves a single twinning plane, as opposed to the predicted three twinning planes that are comprised by a three-layer zonal twinning dislocations. Significantly, atoms in the core zone (enclosed by the white rectangle) appear to be lined up along the twinning plane normal, indicating that the twinning dislocation only carries the parent atoms halfway through (For interpretation of the references to color in this figure legend, the reader is referred to the web version of this article).

3. Results

3.1. Atomic resolution STEM observations

First, the STEM observations are presented and the results are shown in Fig. 2. During cold rolling, $\{11\bar{2}2\}\langle 11\bar{2}\bar{3}\rangle$ twinning was activated. Fig. 2a shows a needle-shaped $\{11\bar{2}2\}$ twin in the parent grain. The $\{11\bar{2}2\}\langle 11\bar{2}\bar{3}\rangle$ twin relationship is confirmed by selected area electron diffraction (SAED) pattern displayed in the inset in which the electron beam is along the $[1\bar{1}00]$. The TB structure is displayed in Fig. 2b and c which are atomic resolution STEM images of the TB. Columns of the basal planes of the parent and twin are clearly resolved when viewed along the zone axis. Careful examinations of the TB reveal that the TB migration only involves a single basal plane at a time, rather than the predicted three basal planes that are comprised in a zonal twinning dislocation [14,15]. In Fig. 2b, at the TB, atoms are being sheared toward the twin positions and this process only involves a single layer of $\{11\bar{2}2\}$ plane, as denoted by the two thin dotted lines. A similar scenario can be observed in Fig. 2c. In this particular case, multiple single layer twinning dislocations are gliding on consecutive twinning planes. when the dislocation lines move near each other, contrast of lattice distortion is created.

The single layer twinning dislocation is better revealed in Fig. 2d, which is a magnified view of the TB. To show that the TB migration only involves one twinning plane at a time, a circuit is drawn around the twinning dislocation core. The solid white line to the right denotes the original position of the TB before migra-

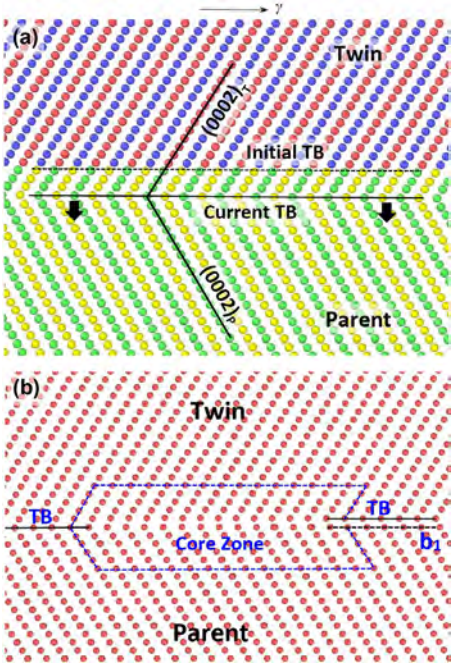

Fig. 3. (a) TB migration under the shear strain. The TB is moving downward. The motion of the TB is accomplished by the lattice transformation from the parent basal plane to the twin basal plane. The green and yellow atoms of the parent are aligned to the basal plane of the twin. Clearly, the second invariant plane K_2 is (0002), rather than the predicted $\{11\bar{2}\bar{4}\}$ or the proposed $\{11\bar{2}\bar{2}\}$. (b) When a circuit is drawn across the TB, it can be seen that the twinning dislocation only involves a single twinning plane, not the predicted three twinning planes. The simulation results are consistent with the atomic resolution STEM observation in Fig. 2 (For interpretation of the references to color in this figure legend, the reader is referred to the web version of this article).

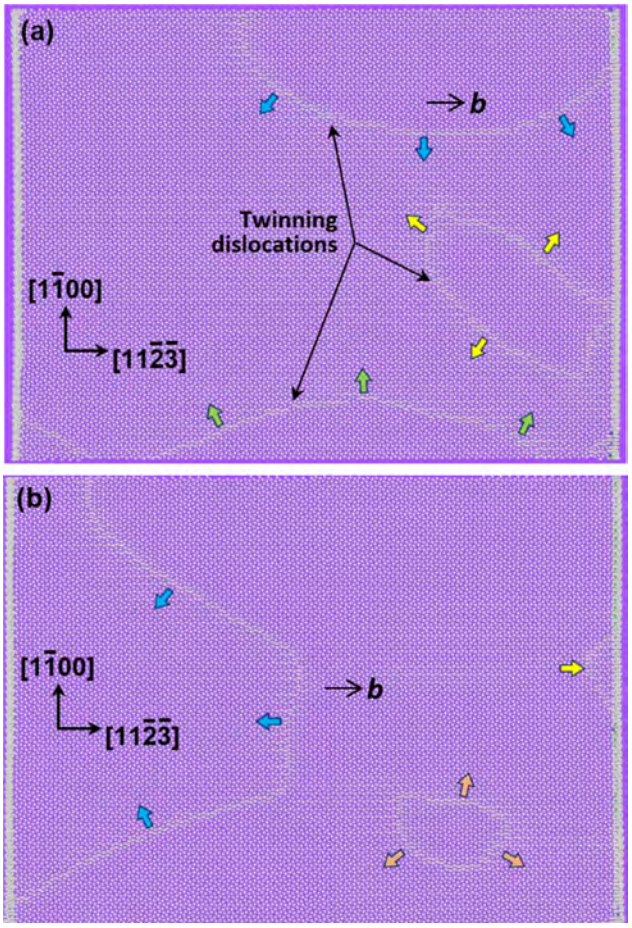

Fig. 4. Twinning dislocation loops nucleated on the twinning plane. The viewing direction is along the normal to the twinning plane. (a) Two dislocation arcs (indicated by the blue and the green arrows) and a loop (indicated by the yellow arrows) are nucleated on the same twinning plane. The dislocations have the same Burgers vector. The arrows indicate the motion of the dislocations. (b) As the dislocation lines and loop approach each other and eventually meet, they merge into a dislocation (indicated by the blue arrows). The other dislocation line is moving out to the free surface as indicated by the yellow arrow. A new dislocation loop (indicated by the brown arrows) is nucleated on the neighboring plane below (For interpretation of the references to color in this figure legend, the reader is referred to the web version of this article).

tion. After the passage of a twinning dislocation, the position of the current TB lies one layer below, which is denoted by the solid white line to the left. For comparison, a white dashed line which is on the same level of the current TB is drawn. Thus, the twinning dislocation only involves a single twinning plane. A salient feature inside the core zone is that the atoms on the slip plane (enclosed by the dotted rectangle) appear to be lined up along the twinning plane normal, strongly suggesting that, although the parent atoms are being sheared toward the twin positions, they are only carried halfway through by the twinning dislocation. In other words, the twinning dislocation only accomplishes half of the total travel distance from the parent position to the twin position. Also, the dislocation core presents a transitional structure which is very different from the core structure of twinning dislocations of other twinning modes. The atoms appear to gradually transition from the parent to the twin rather than are directly sheared to the twin. As analyzed below, this corresponds to the atomic shuffling that accomplishes the other half of the total travel distance.

3.2. Simulation results

Next, the simulation results are presented. How the TB migrates under the shear strain is shown in Fig. 3a which only contains a thin slice (0.5 nm) along the zone axis. The TB migrates downward as the shear strain is increasing. The TB migrates layer by layer, rather than by three layers at a time as predicted by the classical theory. From the color pattern, it can be easily seen that during twinning, the parent basal planes (colored in green and yellow) are transformed to the twin basal planes (colored in red and blue) by the twinning dislocations. After a single-layer twinning dislocation passes through the TB, atoms of parent basal planes are aligned to the twin basal planes. Thus, the parent basal plane (0002) is the second invariant plane K_2, rather than the predicted $\{11\bar{2}\bar{4}\}$.

To show the structure of the twinning dislocation, the color pattern in Fig. 3a is turned off, and only the core zone that shows a transitional structure on the twin boundary is shown. Similarly, a circuit is drawn to demonstrate that indeed, only a single twinning plane is involved in the TB migration. Also, a similar core zone to the atomic resolution STEM image (Fig. 2d) can be observed, although a more compact core zone than that observed in STEM is seen. Inside the core zone, atoms on and below the slip plane appear to be lined up along the normal to the twinning plane and gradually transition to the twin positions.

To better understand the nature of TB migration and the configuration of the twinning dislocations in $\{11\bar{2}2\}\langle 11\bar{2}\bar{3}\rangle$ mode, the projection views of the TB along the normal to the TB plane are plotted and shown in Fig. 4. The evolution of the twinning dislocations is shown in time sequence. In Fig. 4a, various dislocation lines are nucleated on the same twinning plane from the surfaces and then glide inward, as indicated the green and blue arrows. Interestingly, in the same twinning plane, a twinning dislocation loop is also nucleated as indicated by the yellow arrows. These dis-

location lines and loops all have the same Burgers vector and glide in the same slip plane. Thus, as they move toward each other, the dislocations connect and merge, as shown in Fig. 4b. The dislocations on the top and bottom and the dislocation loop merge into a single dislocation moving towards the left surface, as indicated by the blue arrows. Meanwhile, a short dislocation line which is the leftover from the loop is moving out to the right surface (indicated by the yellow arrow). As the dislocations are propagating toward the surfaces, a new dislocation loop (indicated by the brown arrows), which is one layer below, is nucleated and expanding on the neighboring twinning plane. From the morphology of these dislocations, it can be seen that they predominantly have a screw component (the dislocation lines are mostly parallel to the Burgers vector $\boldsymbol{b}$), with short segments of edge component.

Examinations show that each of these dislocation lines and loops entirely lies in a single $\{11\bar{2}2\}$ twinning plane. Thus, they are not the predicted three-layer zonal twinning dislocation. The K_2 plane is not $\{11\bar{2}\bar{2}\}$ proposed by Hall as well. As analyzed below, this K_2 plane would lead to a two-layer zonal twinning dislocation which was not observed in the atomistic simulations.

4. Analysis and discussion

The atomic resolution STEM and MD simulation results in this work show, with clarity, that the K_2 plane of the $\{11\bar{2}2\}\langle 11\bar{2}\bar{3}\rangle$ mode is (0002), indicating that the other K_2 planes, i.e. $\{11\bar{2}\bar{4}\}$ and $\{11\bar{2}\bar{2}\}$ proposed in the literature are unfavorable.

In previous simulations with a smaller system size [21], pairs of dislocation arcs were nucleated and propagated towards free surfaces. As anticipated, when the thickness along the zone axis is doubled, the morphology of the twinning dislocations becomes loops. Thus, irrespective of interatomic potential and system size, only one-layer dislocations and no two-layer or three-layer zonal twinning dislocations are observed. From the crystallography, for a parent atom to travel to the twin position, if the overall displacement solely comes from the one-layer twinning dislocation, the magnitude of the Burgers vector of the twinning dislocation would be [15]:

$$|b| = \frac{a}{\sqrt{1+\gamma^2}} \tag{1}$$

where a is the lattice parameter (0.295 for Ti) and γ the c/a ratio (1.589 for Ti). Thus, $|b| \approx 0.157$ nm. The interplanar spacing d of $\{11\bar{2}2\}$ equals:

$$d = \frac{\gamma \cdot a}{2\sqrt{1+\gamma^2}} \tag{2}$$

Hence, the value of $s = \frac{|b|}{d} = \frac{2}{\gamma} \cdot = \cdot 126$ for Ti [15]. This value is too large for a twinning mode, according to the criterion stated in the classical theory that s should not exceed 1.0.

Li et al. [21] tracked the evolution of the displacement of a pre-selected atom that was far away from the migrating $\{11\bar{2}2\}$ TB on which twinning dislocations were nucleated as paired arcs. It was found that the displacement profile presented a characteristic of stick-slip and the net displacement of the pre-selected atom was actually ~0.08 nm. If the Burgers vector of the twinning dislocation were 0.157 nm, then the net displacement of the pre-selected atom should be 0.157 nm rather than ~0.08 nm. This difference implies that the one-layer twinning dislocation only contributes half of the overall displacement, and the other half comes from shuffling. This analysis is confirmed by the atomic resolution STEM observations in Fig. 2d, for the first time. Therefore, when a parent atom travels and eventually reaches the twin position, only half of the displacement comes from the twinning dislocation glide, and the other half comes from shuffling. Thus, from the STEM observations and the MD simulations, the TB migration can be described as follows: when a twinning dislocation is gliding on its slip plane, it only shears the parent atoms halfway through for ~0.08 nm (Figs. 2d and 3b). This causes the atoms on and below the slip plane to appear to be lined up along the twinning plane normal. After shearing from the twinning dislocation, atoms behind the core zone gradually shuffle toward their twin positions, a process more sluggish than direct shearing. Thus, the fast shearing and sluggish shuffling processes give rise to the twin boundary structure observed in the STEM images (Fig. 2) and in the simulation (Fig. 3).

As stated by Christian [29], shuffling generates no macroscopic effect, because shuffling is only a local atomic activity near the TB in the sense that other atoms far away from the TB do not move along when shuffling occurs. It should be noted that shuffling does generate a macroscopic effect in $\{10\bar{1}2\}\langle 10\bar{1}\bar{1}\rangle$ mode because collective atomic shuffles reorient a parent lattice by nearly 90° and misfit strains are generated between the parent and the twin lattice [32–35]. So more accurately speaking, shuffling generates no macroscopic shear strains. This is different from dislocation glide which is associated with a global displacement that contributes to a global shear strain. From this viewpoint, when the magnitude of twinning shear is calculated, the actual s for the one-layer twinning dislocation should equal $|b|/d \approx 0.66$ rather than 1.26, because the displacement due to shuffling should be excluded from the overall displacement. This analysis properly resolves the conflict between the classical twinning theory which states the value of s should be less than 1.0, and the observed K_2 plane of (0002) in the atomistic simulations.

Previous works reported three possible K_2 planes: $\{11\bar{2}\bar{4}\}$ [1,2,14,15], (0002) [18,21] and $\{11\bar{2}\bar{2}\}$ [16]. As indicated in Fig. 1, when the K_2 plane is determined, then the magnitude of twinning shear and atomic shuffles are determined accordingly. Although various K_2 planes can be selected, only one of them is most plausible. In general, a small s leads to large and complex shuffles [15]. The complexity of shuffles may play a crucial role in determining the actual twinning mechanisms. But there have been insufficient analyses and discussions of atomic shuffles in HCP twinning modes, as a result, the twinning mechanisms remain elusive. In the classical framework of deformation twinning, all the planes of the parent undergo the same homogeneous shear [19]. Planes/vectors of the parent are transformed to the corresponding planes/vectors of the twin. Thus, a one-to-one lattice correspondence can be established between the parent and the twin [29]. As suggested by Christian [15], when a parent atom moves to the twin positions, the overall displacement can be divided into two parts: one part is generated by the homogeneous shear which corresponds to the magnitude of the twinning dislocation, and the other comes from the shuffle that is an extra movement needed to reach the correct twin position. Thus, by following this suggestion, it is possible to perform lattice correspondence analysis so as to identify the shearing and shuffling components. In the following, detailed analyses of lattice correspondences for all the three proposed/observed K_2 planes are provided. Analyses of shuffles for all three K_2 planes are also provided, such that comparison between these proposed twinning mechanisms can be made.

4.1. Lattice correspondence analysis for $K_2 = \{11\bar{2}\bar{4}\}$

For the $K_2=\{11\bar{2}\bar{4}\}$, the magnitude of the Burgers vector of the predicted three-layer zonal twinning dislocation b_3 equals [15]:

$$|b_3| = \frac{\left(\gamma^2-2\right)\cdot a}{\sqrt{1+\gamma^2}} \tag{3}$$

which is about 0.082 nm for Ti. Thus, on each of the three twinning planes that are comprised in the zonal twinning dislocation,

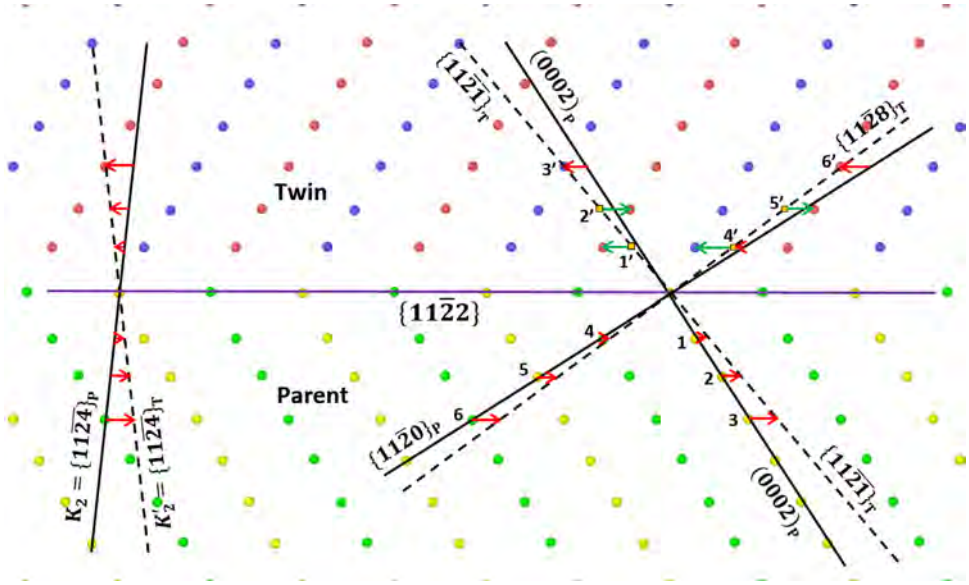

Fig. 5. Lattice correspondence analysis when the K_2 plane is $\{11\bar{2}\bar{4}\}$. The components of the shuffles are in the plane of shear. To the left, three red arrows represent the homogeneous shear on three consecutive twinning planes. To the right, a parent basal plane experiences the same homogeneous shear as does the K_2 plane. Three atoms on the basal plane are selected: 1, 2 and 3. The homogeneous shear carries atom 1 and 2 to 1′ and 2′ which are represented by the square yellow symbols. But position 1′ and 2′ are not on the twin lattice and shuffles are needed (indicated by the green arrows). No shuffling is needed for atom 3. The shear and shuffle transform the parent basal to three successive $\{11\bar{2}\bar{1}\}$ planes of the twin. Similarly, a parent $\{11\bar{2}0\}$ plane is transformed to three consecutive $\{11\bar{2}8\}$ planes of the twin (For interpretation of the references to color in this figure legend, the reader is referred to the web version of this article).

the displacement generated by shearing is about 0.027 nm. For this three-layer zonal twinning dislocation, the corresponding s equals [15]:

$$s = \frac{2\left(\gamma^2 - 2\right)}{3\gamma} \approx 0.22 \tag{4}$$

How the homogeneous shear and shuffles transform the parent lattice into the twin lattice is shown in Fig. 5. The K_2 plane intersects the $\{11\bar{2}2\}$ twinning planes at a lattice point every three layers from the TB. Thus, this dislocation should simultaneously comprise three consecutive $\{11\bar{2}2\}$ planes [36–39,15]. To the left of Fig. 5, the trace of the K_2=$\{11\bar{2}\bar{4}\}$ is denoted by the solid black line. The array of three red arrows represents the homogeneous shear which shears the parent K_2 plane to the position denoted by the dashed black line. This dashed line exactly falls on the position of $K_2' = \{11\bar{2}\bar{4}\}$ of the twin. Thus, no distortion is produced on this plane, i.e. invariant. It is obvious that, atoms at every third layer are carried directly to the twin positions without the need of atomic shuffling.

To the right of Fig. 5, transformations of (0002) and $\{11\bar{2}0\}$ of the parent lattice are analyzed, to demonstrate the one-to-one lattice correspondence. Because the homogeneous shear that invariantly transforms the K_2 to the K_2' is an affine shear [15], each atoms of the parent basal plane must undergo the same homogeneous shear. Three atoms 1, 2, and 3 on the parent plane are selected for the analysis of shear and shuffle. After the homogeneous shear, these atoms are affinely sheared to three positions on the dashed line. From the twin symmetry, these positions are then reflected to the equivalent positions 1′, 2′ and 3′ in the twin. These positions are now compared with the actual twin positions. For atom 3, it is obvious that it is directly sheared to the twin position 3′ without the need of shuffling. For atom 1 and 2, the reflected positions 1′ and 2′, which are denoted by the yellow square symbols on the dashed line, are obviously not on the twin positions. This indicates that atomic shuffling is needed for these two atoms to reach the twin positions. The shuffles are denoted by the green arrows. For position 1′, the direction of shuffling goes along the direction of the twinning shear; for position 2′, the direction of shuffling goes against the direction of the twinning shear. Note that these are only the shuffling components inside the plane of shear, i.e. the plane perpendicular to the K_1, K_2 and the zone axis. The shuffling components that are out of the plane of shear will be analyzed below. After the homogeneous shear and the shuffles, atom 1 and 2 reach the twin positions. Crystallographic examination shows that after shuffling, position 1′, 2′ and 3′ are adjusted to three positions that fall on three consecutive $\{11\bar{2}\bar{1}\}$ planes of the twin. In other words, a single (0002) basal plane of the parent is transformed to three consecutive $\{11\bar{2}\bar{1}\}$ planes of the twin. This can be seen from the fact that the dashed line is exactly the trace of $\{11\bar{2}\bar{1}\}$ plane of the twin on which position 3′ resides. The net effect of the shear and shuffle produces the lattice correspondence that can be described as: $(0002)_P \rightarrow \{11\bar{2}\bar{1}\}_T$.

Similar lattice correspondence analysis can be conducted for $\{11\bar{2}0\}$ plane of the parent, i.e. the second order prismatic plane. In Fig. 5, atoms 4, 5 and 6 are selected to show the lattice transformation. The array of three red arrows represent the homogeneous simple shear on three consecutive twinning planes, which carry these atoms to positions 4′, 5′ and 6′ on the dashed black line. But positions 4′ and 5′ do not fall on the twin positions, and only position 6′ does. Thus, shuffles are required for atoms 4 and 5, as indicated by the green arrows. For atom 4, it has to shuffle along the direction of twinning shear; for atom 5, it has to shuffle against the direction of twinning shear. The dashed black line can be identified as the trace of $\{11\bar{2}8\}$ plane of the twin. Thus, the shear and shuffle transform a single-layer $\{11\bar{2}0\}$ plane of the parent into three consecutive $\{11\bar{2}8\}$ planes of the twin. This transformation can be described as: $\{11\bar{2}0\}_P \rightarrow \{11\bar{2}8\}_T$.

The above lattice correspondence analyses indicate that, if the K_2 plane is $\{11\bar{2}\bar{4}\}$ as predicted in the classical theory, atoms on a (0002) plane of the parent must reside on three consecutive $\{11\bar{2}\bar{1}\}$ planes of the twin after twinning, and those atoms on a $\{11\bar{2}0\}$ plane of the parent must reside on three consecutive $\{11\bar{2}8\}$ planes of the twin. These transformations inevitably entail large shuffles such that the parent atoms can reach the twin positions and accomplish the lattice transformation. The analyses in Fig. 5 can be used to estimate the magnitude of shuffling in the plane of shear,

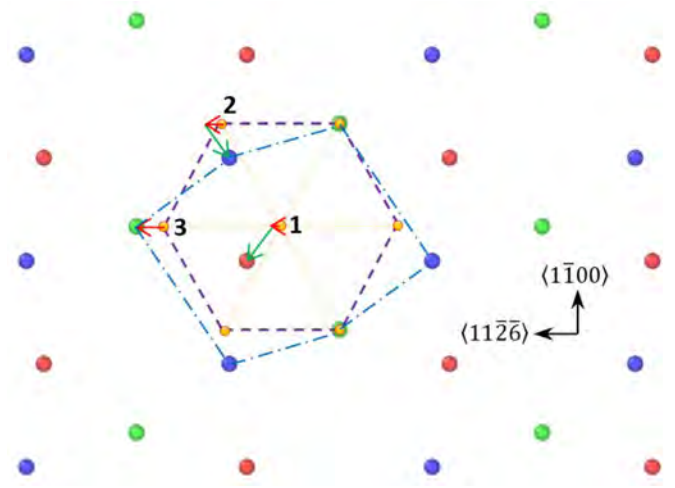

Fig. 6. Components of the shuffles that are off the plane of shear when the K_2 plane is $\{11\bar{2}\bar{4}\}$. A basal plane (denoted by the yellow atoms and the purple dashed lines) is transformed to three consecutive $\{11\bar{2}\bar{1}\}$ planes (red/blue/green atoms) of the twin. The structural motif is denoted by the dot-dashed blue lines. The basal hexagon of the parent is transformed to the motif of the corresponding $\{11\bar{2}\bar{1}\}$ planes of the twin. The viewing direction is along the normal to the $\{11\bar{2}\bar{1}\}$ plane. The shuffling components along the $\langle 1\bar{1}00\rangle$ direction can now be seen. After shear (indicated by the red arrows), large shuffles at position 1 and 2 (indicated by the green arrows) are needed to reach the twin lattice (cf. Fig. 5). Atom 3 is directly sheared to the twin position and no shuffle is needed. The shear and shuffle result in a large distortion to the motif (For interpretation of the references to color in this figure legend, the reader is referred to the web version of this article).

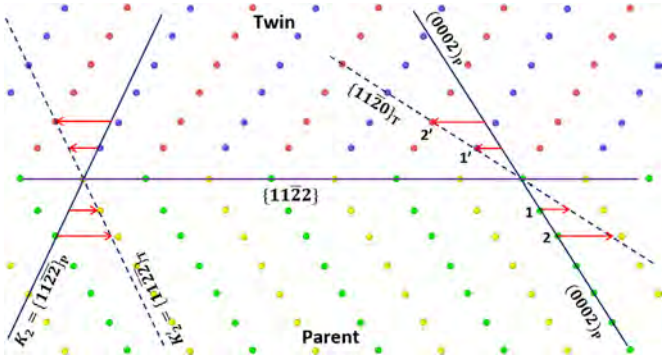

Fig. 7. Lattice correspondence analysis when the K_2 plane is $\{11\bar{2}\bar{2}\}$. The twinning plane intersects with the K_2 plane at a lattice point every two layers and the twinning dislocation is a two-layer zonal. The parent basal plane (0002) is transformed to the $\{11\bar{2}0\}$ of the twin. Two atoms 1 and 2 are selected to analyze the lattice transformation. Shuffling is needed for atom 1 but not for atom 2. The value of s equals 0.96 for Ti, which is close to 1.0.

for instance, the maximum distance of shuffling in the plane of shear can be taken as the net displacement after the shearing displacement is excluded from the overall displacement from the parent to twin. For atom 1, this equals ~0.074 nm. As analyzed above, the net displacement caused by a zonal twinning dislocation on each twinning plane is ~0.027 nm, which is only about one-third of the displacement caused by shuffling. Thus, large shuffles are needed if the K_2 plane is $\{11\bar{2}\bar{4}\}$. The shuffles shown in Fig. 5, however, do not include the components in the direction perpendicular to the direction of twinning shear, and these components are analyzed as follows.

To reveal the shuffling components off the plane of shear, the structure of a parent basal plane and its corresponding plane of the twin, $\{11\bar{2}\bar{1}\}$ in this case are compared. In Fig. 6, first a basal plane is plotted, as indicated by the dashed purple lines connecting the yellow atoms. Then three neighboring $\{11\bar{2}\bar{1}\}$ planes are plotted, each plane is displayed as red, green and blue, respectively. Only the transformation of the parent basal plane is analyzed, but similar analysis can be performed for the transformation of $\{11\bar{2}0\}$ plane as well. The viewing direction is along the normal direction of the $\{11\bar{2}\bar{1}\}$ plane. Now the basal plane and three $\{11\bar{2}\bar{1}\}$ planes are superimposed such that the lattice points along the zone axis $[1\bar{1}00]$ are perfectly matched. Immediately, the shuffling components out of the plane of shear, i.e. the components along $[1\bar{1}00]$ can be resolved. Three atoms of the parent basal plane, 1, 2 and 3 are selected, and they correspond to atom 1, 2 and 3 in Fig. 5. Three red arrows represent the homogeneous simple shear along the twinning direction. It can be seen that, for atom 3, it is directly sheared to the twin position without the need of shuffling. For atom 1 and 2, additional shuffling components off the shearing direction are needed. As indicated by the green arrows, atom 1 has to shuffle downward to reach the twin position (the red atom position); atom 2 has to shuffle downward as well to reach the twin position (the blue atom position). The magnitude of these shuffles are much larger than the displacement incurred by the twinning shear. Clearly, the basal plane have to experience large and complex shuffles such that a parent basal plane is transformed to three successive $\{11\bar{2}\bar{1}\}$ planes of the twin. Atom 1 and 2 have to shuffle along opposite directions. Such a complex pattern of large shuffles is not structurally and energetically favorable for a twinning mode. Thus, $\{11\bar{2}\bar{4}\}$ is not a plausible K_2 plane for $\{11\bar{2}2\}\langle 11\bar{2}\bar{3}\rangle$ twinning mode.

In Fig. 6, a distorted hexagon is delineated by the dash-dotted blue lines. This is the structural motif as a product of the lattice transformation from the symmetric basal hexagon which is the structural motif of the parent basal plane. The comparison between these two motifs provides a clear illustration in terms of the magnitude of the shear and the complexity of the shuffles in $\{11\bar{2}2\}\langle 11\bar{2}\bar{3}\rangle$ twinning if the K_2 plane is $\{11\bar{2}\bar{4}\}$. Christian and Mahajan [15] stated that "rather complex" shuffles are required for this twinning mode if the K_2 is $\{11\bar{2}\bar{4}\}$. Now all the shuffling components are revealed. Indeed, to transform the hexagon of the parent basal plane to the distorted hexagon that is connected to three consecutive $\{11\bar{2}\bar{1}\}$ planes of the twin, very perhaps prohibitively complex shuffles are needed.

4.2. Lattice correspondence analysis for $K_2 = \{11\bar{2}\bar{2}\}$

The $K_2 = \{11\bar{2}\bar{4}\}$ generates a value of $s \approx 0.22$ which is small but requires a three-layer zonal twinning dislocation with large and complex shuffles (Figs. 5 and 6). Hall [16] suggested an alternative K_2 plane, $\{11\bar{2}\bar{2}\}$ [15]. The value of s for this particular K_2 plane equals:

$$s = \gamma - \gamma^{-1} \tag{5}$$

For Ti, $s = 0.96$, which is close to 1.0, but only half of the parent atoms need shuffling (see analysis below). The lattice correspondence analysis is shown in Fig. 7. The K_2 plane (indicated by the solid black line) intersects the twinning planes at a lattice point every two layers from the TB plane. Hence, the twinning dislocation should comprise two neighboring planes simultaneously, i.e. a two-layer zonal twinning dislocation. The Burgers vector of the two-layer zonal twinning dislocation equals

$$b_2 = \frac{\left(\gamma - \gamma^{-1}\right) \cdot \gamma \cdot a}{\sqrt{1+\gamma^2}} \tag{6}$$

To the left of Fig. 7, the homogeneous simple shear is represented by the solid red arrows on the two neighboring twinning planes. The red arrows homogeneously shear the K_2 plane of the parent (denoted by the solid black line) to the new position which is exactly the K_2' plane of the twin. To the right, two

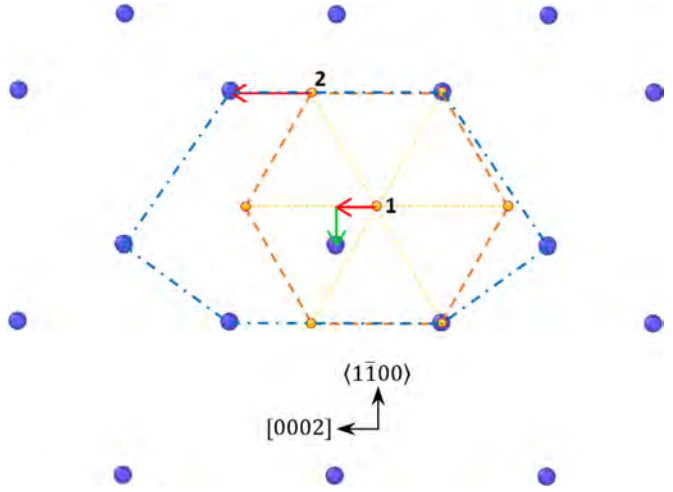

Fig. 8. Lattice correspondence analysis when the K_2 plane is $\{11\bar{2}\bar{2}\}$ [16]. The viewing direction is along the normal of the $\{11\bar{2}0\}$ plane represented by the blue atoms. The parent basal plane (0002) (denoted by the yellow atoms and the dashed brown lines) is transformed to the $\{11\bar{2}0\}$ of the twin. The structural motif of the twin is denoted by the dot-dashed blue lines. The basal hexagon, i.e. the structural motif of the parent is transformed to the motif of the corresponding $\{11\bar{2}0\}$ plane of the twin. Atom 1 has to shuffle downward to reach the twin position after shear. Atom 2 is directly sheared to the twin position without the need of shuffle. The shear and shuffle result in a large distortion to the motif (For interpretation of the references to color in this figure legend, the reader is referred to the web version of this article).

atoms 1 and 2 on the parent basal plane undergo the same homogeneous shear. After shearing, the positions of atom 1 and 2 are reflected to the positions in the twin. Now it is clear that atom 2 is directly sheared to the twin position 2′ (in red), thus no shuffling is needed for this atom. In contrast, atom 1 is carried by shearing to position 1′ in the twin which is seemingly a twin position (the blue atom) but actually not. This is because position 1′ and the blue atom actually lie in two separate planes that are parallel to the plane of shear (see Fig. 8 below). After shearing and shuffling, it can be seen that the parent basal is transformed to the $\{11\bar{2}0\}$ plane of the twin. The lattice correspondence can be described as $(0002)_P \rightarrow \{11\bar{2}0\}_T$. Reciprocally, the $\{11\bar{2}0\}$ plane of the parent is obviously transformed to the basal plane of the twin.

To better visualize how the lattice transformation $(0002)_P \rightarrow \{11\bar{2}0\}_T$ is accomplished, a projection view of the $\{11\bar{2}0\}$ plane is plotted and shown in Fig. 8. The viewing direction is along the normal of $\{11\bar{2}0\}$ plane, i.e. $\langle 11\bar{2}0\rangle$. The atoms on this plane are shown in blue. On top of this plot, a basal hexagon is superimposed. The basal hexagon is denoted by the dashed purple lines and the small yellow atoms. Atoms 1 and 2, which correspond to atoms 1 and 2 in Fig. 7 are selected for the analysis. The red arrows attached to atoms 1 and 2 represent the homogeneous simple shear. For atom 1, the shear cannot carry it to the twin position. It has to shuffle downward to reach the twin position. The magnitude of the shuffle is ~0.085 nm. For atom 2, it is directly sheared to the twin position and no shuffle is needed.

In Fig. 8, a distorted hexagon on the $\{11\bar{2}0\}$ plane is delineated by the dash-dotted blue lines that connect the blue atoms. This is the structural motif as a product of the shear and shuffle that are undergone by the symmetric hexagon of the parent basal plane, and the distortion is significant. Therefore, although half of the parent atoms can be directly carried to the twin positions by the shear and only half of the parent atoms need shuffles, the large value of s is unfavorable as well when the K_2 plane is $\{11\bar{2}\bar{2}\}$. This is probably the reason why this mechanism has not been observed in atomistic simulations.

4.3. Lattice correspondence analysis for $K_2 = (0002)$

The shear and shuffle when $K_2 = (0002)$ was partly analyzed in [24] but the analysis was incomplete. From the perspective of lattice correspondence, crystallographically the $K_2 = (0002)$ results in a simplest lattice transformation because no distortion is produced in the structural motif. The basal hexagon experiences no distortion after twinning. However, as shown in Figs. 2d and 3b, if no shuffling was involved during twinning, for $K_2 = (0002)$ the twinning shear would equal $s = 2/\gamma$. For Ti, the s equals 1.26. This s is implausibly large [15] if all the parent atoms are carried to the twin lattice solely by the single-layer twinning dislocation without shuffling. The STEM observations and simulation results in this work, along with other simulations [18,21] reveal that the actual K_2 plane is indeed (0002). The answer to this conflict lies in the fact shuffling is actually involved in the lattice transformation [24], as shown in the STEM observations (Fig. 2d). Fig. 9 shows the lattice correspondence analysis when $K_2 = (0002)$. The parent basal plane, i.e. the K_2 plane (indicated by the solid black line), is transformed to the basal plane of the twin (indicated by the dashed black line). However, the lattice transformation is not accomplished all by shear, instead, it is accomplished half by shear and half by shuffle. As shown in the inset, the atoms of the parent basal are first carried to an intermediate position (indicated by the double dot-dashed line) by the single-layer twinning dislocation which has a magnitude of the Burgers vector of ~0.08 nm. Then the rest of the journey is completed by shuffling. The magnitude of the shuffle is nearly equal to that of the twinning dislocation. The shear and the shuffle are denoted by the red and the green arrows, respectively. As such, the magnitude of twinning shear is reduced.

Fig. 10 shows a projection view of the shear and shuffle, along the normal to the $\{11\bar{2}2\}$ twinning plane. Three consecutive twinning planes are plotted in different colors: from top down, red, yellow and green. The half-shear-half-shuffle process can be better represented and rationalized. Under the shear stress, the red atoms of the parent are first sheared to the midpoint between the two yellow atoms (indicated by the red arrow). Thus, the parent atoms reach an intermediate position (Fig. 2d), and this step of shearing produces the magnitude of twinning shear ($s \approx 0.66$) along the twinning direction. This step also produces the unique transitional structure as revealed in the STEM observations and the atomistic simulations (Figs. 2d and 3b), in which the atoms in the core zone appear to be lined up along the twinning plane normal. Second, the red atoms shuffle to the twin position (indicated by the green arrow). This distance of shuffling is about 0.08 nm, but it makes no contribution to s. Thus, the whole process can be divided into two steps. In this two-step twinning process, the atoms move all along the direction of the twinning shear, there is no need for complex atomic movements in the opposite directions or against the direction of twinning shear or off the plane of shear, and the magnitudes of shear and shuffle are not unrealistically large. This makes the migration of the TB not difficult to realize.

After shear and shuffle, the red and the green layers are now mirrored about the yellow layer, but the actual value of s equals ~0.66 rather than 1.26. This magnitude of twinning shear, along with the very simple shuffle if compared with the shuffles in the other K_2 planes, is much more plausible and favorable, because: (1) Only a simple shuffle that is along the direction of twinning shear is involved; (2) Conceivably, zonal twinning dislocations which simultaneously comprise multiple twinning planes and require complex shuffles are not energetically and structurally favorable. For the single-layer twinning dislocation that only comprises one twinning plane, it is much easier to be activated.

The above analyses for all three K_2 planes are consistent with the general description in the classical twinning theory:

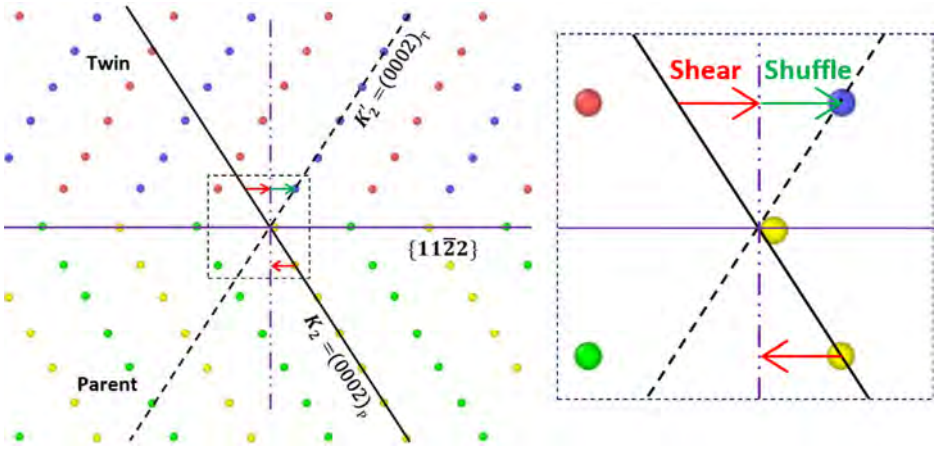

Fig. 9. Lattice correspondence analysis when the K_2 plane is (0002). As shown in Fig. 2a, the parent basal is transformed to the twin basal. The inset to the right shows that, the atoms of the parent basal are not carried to the twin positions by the homogeneous shear alone; instead, they are sheared by a twinning Burgers vector of ~0.08 nm along the twinning direction (indicated by the red arrows), then the rest of the journey is accomplished by shuffling (indicated by the green arrow). This process significantly reduces the overall magnitude of twinning shear (For interpretation of the references to color in this figure legend, the reader is referred to the web version of this article).

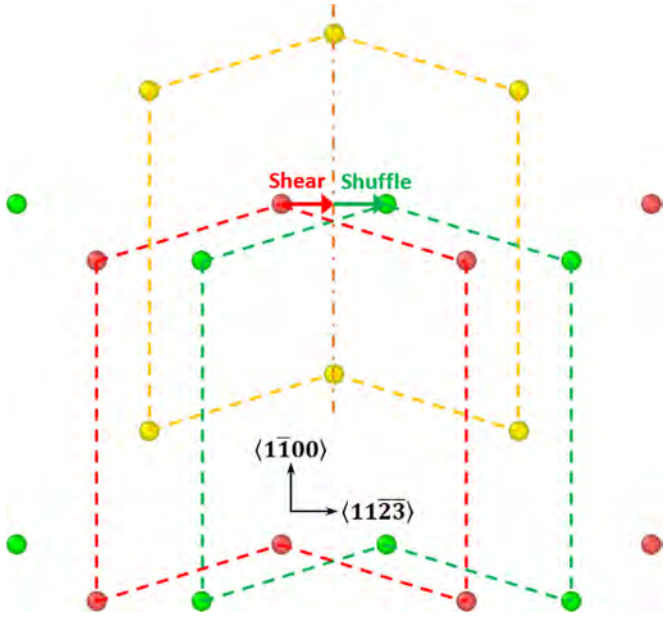

Fig. 10. Shear and shuffle on the $\{11\bar{2}2\}$ twinning plane when the K_2 plane is (0002). The viewing direction is along the normal of the twinning plane. Three consecutive twinning planes are shown: from top down, red, yellow and green. The red layer is being displaced over the yellow layer, such that eventually the red and the green layers are mirrored about the yellow layer. This process is accomplished half by shear (indicated by the red arrow) and half by shuffle (indicated by the green arrow)(For interpretation of the references to color in this figure legend, the reader is referred to the web version of this article).

the requirement of a small magnitude of twinning shear and the requirement of simple shuffles work at odds with each other. The smaller the magnitude of twinning shear, the more complex atomic shuffles are required. The (0002) K_2 plane, which has been observed in the STEM and atomistic simulations, is a good compromise to satisfy these two requirements.

Even with the reduced value of s (~0.66) for K_2 = (0002), this value is still much larger than the experimentally measured s (~0.22). To resolve this conflict, it is important to realize that interferometry, a technique that was used to measure s, is very sensitive to surface condition. As pointed out by Christian [15], to accurately measure s is not easy, because accommodation effects may come into play and lead to significant errors. For one example, the measured s for $\{11\bar{2}1\}\langle 11\bar{2}\bar{6}\rangle$ mode in Zr [1] was ~0.22, but the theoretical value of s, which equals $\frac{1}{\gamma}$, should be 0.64 [15]. As suggested by Christian and Mahajan [15], accommodation effects were likely the source of inaccuracy. The measured small $s \approx$ 0.22 for $\{11\bar{2}2\}\langle 11\bar{2}\bar{3}\rangle$ mode could also be a result of accommodation effects such as surface relief, twin-slip, twin-twin interaction etc. [15].

The above lattice correspondence analyses on three possible K_2 planes for $\{11\bar{2}2\}\langle 11\bar{2}\bar{3}\rangle$ twinning mode, which are performed inside the framework of the classical twinning theory, underscore why it is crucially important to conduct such analyses for all the twinning modes in HCP metals. Thus, the predicted K_2=$\{11\bar{2}\bar{4}\}$, which has been widely accepted, is likely incorrect. It is worth noting that, this does not necessarily indicate that the classical twinning theory fails to properly describe the twinning modes in HCP metals. On the contrary, it is demonstrated in this work that, by performing lattice correspondence analyses inside the classical framework of deformation twinning, one is able to identify the most plausible twinning elements for a twinning mode with the assistance of carefully conducted experiments and atomistic simulations. Such analyses would be very difficult without the aid of computer simulations. It is fair to conclude that in general, the classical theory works well and is able to solve twinning problems in HCP and other crystal structures, if properly applied.

5. Conclusion

In this work, $\{11\bar{2}2\}\langle 11\bar{2}\bar{3}\rangle$ TB structure and migration were investigated by STEM combined with atomistic simulations. The experimental observations and atomic scale simulations agree very well. The following conclusions can be reached:

(1) Both STEM observations and atomistic simulations reveal that the TB migration is mediated by twinning dislocations which only involve a single $\{11\bar{2}2\}$ twinning plane, not the predicted zonal twinning dislocations which simultaneously comprise three twinning planes. The STEM observations clearly resolve a core structure that is quite different from that of twinning dislocations of other twinning modes in which a homogeneous shear dominates the action. The parent atoms are sheared by the twinning dislocation halfway through, and the rest of the travel is accomplished by shuffling gradually.
(2) In the half-shear-half-shuffle twinning process, parent atoms are first sheared to the intermediate positions by the twinning

dislocation, then gradually transition to the twin positions by shuffling. Thus, the overall magnitude of twinning shear is reduced and equals ~0.66, instead of 1.26. Thus, the conflict between the classical theory, atomistic simulations, experimental measurements and observations can now be reconciled.

(3) In the simulations, the twinning dislocations can be nucleated as dislocation loops on the twinning plane. The second invariant plane, i.e. the K_2 plane is (0002), not $\{11\bar{2}\bar{4}\}$ as predicted in the classical twinning theory. During twinning, the (0002) basal plane of the parent is transformed to the basal plane of the twin. This lattice transformation involves a homogeneous shear and a simple shuffle along the direction of twinning shear, making this K_2 plane favorable.

(4) The lattice correspondence analyses for all three possible K_2 planes reveal that the predicted $K_2=\{11\bar{2}\bar{4}\}$ would require very complex shuffles. Some atoms would have to shuffle against the direction of twinning shear and off the plane of shear. The shuffling displacement would be much larger than the shear displacement incurred by the twinning shear on each of the three twinning planes. The small twinning shear and the complex shuffles would transform a basal plane of the parent into three consecutive $\{11\bar{2}\bar{1}\}$ planes of the twin, causing large distortion to the structural motif. For the $K_2=\{11\bar{2}\bar{2}\}$, the value of s is large. A shuffle off the plane of shear would also be required, and a large distortion to the structural motif would be incurred. Thus, both $K_2=\{11\bar{2}\bar{4}\}$ and $K_2=\{11\bar{2}\bar{2}\}$ are unfavorable. The $K_2 = (0002)$ which was obtained in the STEM observation and simulation is most plausible.

Declaration of Competing Interest

The authors declare that they have no known competing financial interests or personal relationships that could have appeared to influence the work reported in this paper.

Acknowledgments

Manling Sui thanks the financial supports from the National Natural Science Foundation of China (Nos. 11374028 and U1330112), the Scientific Research Key Program of Beijing Municipal Commission of Education (No. KZ201310005002), Beijing Municipal Found for Scientific Innovation (PXM2019_014204s_500031), Foundation on the Creative Research Team Construction Promotion Project of Beijing Municipal Institution (IDHT20190503). Bin Li gratefully thanks the support from U.S. National Science Foundation (CMMI-2016263, 2032483).

References

[1] E.J. Rapperport, Room temperature deformation processes in zirconium, Acta Metall. 7 (1959) 254–260, doi:10.1016/0001-6160(59)90018-5.
[2] N.E. Paton, W.A. Backofen, Plastic deformation of titanium at elevated temperatures, Metall. Trans. 1 (1970) 2839–2847.
[3] F. Xu, X. Zhang, H. Ni, Q. Liu, Deformation twinning in pure Ti during dynamic plastic deformation, Mater. Sci. Eng. A 541 (2012) 190–195, doi:10.1016/j.msea.2012.02.021.
[4] N. Bozzolo, L. Chan, A.D. Rollett, Misorientations induced by deformation twinning in titanium, J. Appl. Crystallogr. 43 (2010) 596–602, doi:10.1107/S0021889810008228.
[5] T.A. Mason, J.F. Bingert, G.C. Kaschner, S.I. Wright, R.J. Larsen, Advances in deformation twin characterization using electron backscattered diffraction data, Metall. Mater. Trans. A 33 (2002) 949–954, doi:10.1007/s11661-002-0164-8.
[6] X. Li, Y.L. Duan, G.F. Xu, X.Y. Peng, C. Dai, L.G. Zhang, Z. Li, EBSD characterization of twinning in cold-rolled CP-Ti, Mater. Charact. 84 (2013) 41–47, doi:10.1016/j.matchar.2013.07.008.
[7] M.H. Yoo, Slip, twinning, and fracture in hexagonal close-packed metals, Metall. Trans. A 12 (1981) 409–418, doi:10.1007/BF02648537.
[8] B.M. Morrow, R.J. McCabe, E.K. Cerreta, C.N. Tomé, Observations of the atomic structure of tensile and compressive twin boundaries and twin–twin interactions in zirconium, Metall. Mater. Trans. A 45 (2014) 5891–5897, doi:10.1007/s11661-014-2481-0.
[9] Y. Guo, J. Schwiedrzik, J. Michler, X. Maeder, On the nucleation and growth of $\{112\bar{}2\}$ twin in commercial purity titanium: *in situ* investigation of the local stress field and dislocation density distribution, Acta Mater. 120 (2016) 292–301, doi:10.1016/j.actamat.2016.08.073.
[10] Y. Guo, H. Abdolvand, T.B. Britton, A.J. Wilkinson, Growth of $\{112\bar{}2\}$ twins in titanium: a combined experimental and modelling investigation of the local state of deformation, Acta Mater. 126 (2017) 221–235, doi:10.1016/j.actamat.2016.12.066.
[11] C. Cayron, The (11-22) and (-12-16) twinning modes modelled by obliquity correction of a (58deg, a+2b) prototype stretch twin, Acta Crystallogr. Sect. Found. Adv. 74 (2018) 44–53, doi:10.1107/S2053273317015042.
[12] P. Ye, J. Yao, B. Wang, H. Liu, L. Deng, C. Wang, J. Chen, Q. Li, A comparative study between {11−22} twinning and {10−12} twinning variant selection mechanisms during uniaxial compression in pure titanium, Mater. Charact. 162 (2020) 110188, doi:10.1016/j.matchar.2020.110188.
[13] Q. Yu, Z.W. Shan, J. Li, X. Huang, L. Xiao, J. Sun, E. Ma, Strong crystal size effect on deformation twinning, Nature 463 (2010) 335–338, doi:10.1038/nature08692.
[14] B.A. Bilby, A.G. Crocker, The Theory of the crystallography of deformation twinning, Proc. R. Soc. Math. Phys. Eng. Sci. 288 (1965) 240–255, doi:10.1098/rspa.1965.0216.
[15] J.W. Christian, S. Mahajan, Deformation twinning, Prog. Mater. Sci. 39 (1995) 1–157, doi:10.1016/0079-6425(94)00007-7.
[16] E.O. Hall, Twinning and Diffusionless Transformations in Metals, Butterworth, London, 1954.
[17] A. Serra, D.J. Bacon, R.C. Pond, Twins as barriers to basal slip in hexagonal-close-packed metals, Metall. Mater. Trans. A 33 (2002) 809–812, doi:10.1007/s11661-002-0149-7.
[18] A. Serra, D.J. Bacon, Modelling the motion of {1122} twinning dislocations in the HCP metals, Mater. Sci. Eng. A 400–401 (2005) 496–498, doi:10.1016/j.msea.2005.01.067.
[19] R. Abbaschian, L. Abbaschian, R.E. Reed-Hill, Physical Metallurgy Principles, 4th Ed., Cengage Learning India, 2008.
[20] D.G. Westlake, Twinning in zirconium, Acta Metall. 9 (1961) 327–331, doi:10.1016/0001-6160(61)90226-7.
[21] B. Li, H. El Kadiri, M.F. Horstemeyer, Extended zonal dislocations mediating twinning in titanium, Philos. Mag. 92 (2012) 1006–1022, doi:10.1080/14786435.2011.637985.
[22] A. Serra, D.J. Bacon, R.C. Pond, A comment on B. Li, H. El Kadiri and M.F. Horstemeyer 'Extended zonal dislocations mediating twinning in titanium, Philos. Mag. 93 (2013) 3495–3503, doi:10.1080/14786435.2013.815816.
[23] H.E. Kadiri, C.D. Barrett, Comments on "extended zonal dislocations mediating twinning in titanium, Philos. Mag. 93 (2013) 3491–3494, doi:10.1080/14786435.2013.815815.
[24] B. Li, Reply to the two Comments, by, A. Serra, D.J. Bacon and R.C. Pond, and by H. El Kadiri and C. Barrett on B. Li, H. El Kadiri and M.F. Horstemeyer "Extended zonal dislocations mediating twinning in titanium, Philos. Mag. 93 (2013) 3504–3510, doi:10.1080/14786435.2013.815818.
[25] R.R. Zope, Y. Mishin, Interatomic potentials for atomistic simulations of the Ti-Al system, Phys. Rev. B 68 (2003) 024102, doi:10.1103/PhysRevB.68.024102.
[26] M.S. Daw, M.I. Baskes, Semiempirical, Quantum mechanical calculation of hydrogen embrittlement in metals, Phys. Rev. Lett. 50 (1983) 1285–1288, doi:10.1103/PhysRevLett.50.1285.
[27] M.S. Daw, M.I. Baskes, Embedded-atom method: derivation and application to impurities, surfaces, and other defects in metals, Phys. Rev. B 29 (1984) 6443–6453, doi:10.1103/PhysRevB.29.6443.
[28] M. Niewczas, Lattice correspondence during twinning in hexagonal close-packed crystals, Acta Mater. 58 (2010) 5848–5857, doi:10.1016/j.actamat.2010.06.059.
[29] J.W. Christian, The Theory of Transformations in Metals and Alloys, Newnes, 2002.
[30] S. Nosé, A unified formulation of the constant temperature molecular dynamics methods, J. Chem. Phys. 81 (1984) 511–519, doi:10.1063/1.447334.
[31] W.G. Hoover, Canonical dynamics: equilibrium phase-space distributions, Phys. Rev. A 31 (1985) 1695–1697, doi:10.1103/PhysRevA.31.1695.
[32] B. Li, E. Ma, Atomic shuffling dominated mechanism for deformation twinning in magnesium, Phys. Rev. Lett. 103 (2009) 035503, doi:10.1103/PhysRevLett.103.035503.
[33] B. Li, X.Y. Zhang, Global strain generated by shuffling-dominated twinning, Scr. Mater. 71 (2014) 45–48, doi:10.1016/j.scriptamat.2013.10.002.
[34] B. Li, X.Y. Zhang, Twinning with zero twinning shear, Scr. Mater. 125 (2016) 73–79, doi:10.1016/j.scriptamat.2016.07.004.
[35] J. Wang, S.K. Yadav, J.P. Hirth, C.N. Tomé, I.J. Beyerlein, Pure-shuffle nucleation of deformation twins in hexagonal-close-packed metals, Mater. Res. Lett. 1 (2013) 126–132, doi:10.1080/21663831.2013.792019.
[36] S. Mendelson, Zonal dislocations and twin lamellae in h.c.p. metals, Mater. Sci. Eng. 4 (1969) 231–242, doi:10.1016/0025-5416(69)90067-6.
[37] S. Mendelson, Dissociations in HCP metals, J. Appl. Phys. 41 (1970) 1893–1910, doi:10.1063/1.1659139.
[38] M.L. Kronberg, A structural mechanism for the twinning process on $\{101^2\}$ in hexagonal close packed metals, Acta Metall. 16 (1968) 29–34, doi:10.1016/0001-6160(68)90068-0.
[39] A.L. Lann, A. Dubertret, A development of Kronberg's model for 1012 twins in H.C.P. metals. Extension to 1122 twins, Phys. Status Solidi A 51 (2021) 497–507, doi:10.1002/pssa.2210510223.